Nuclear Engineering and Design 335 (2018) 128–139

Contents lists available at ScienceDirect

Nuclear Engineering and Design

journal homepage: www.elsevier.com/locate/nucengdes

Ultimate pressure capacity of nuclear reactor containment buildings under unaged and aged conditions

Sara Alhanaee[a], Yongsun Yi[b,*], Andreas Schiffer[c]

[a] Federal Authority for Nuclear Regulation, Abu Dhabi, United Arab Emirates
[b] Nuclear Engineering, Khalifa University of Science and Technology, Abu Dhabi, United Arab Emirates
[c] Mechanical Engineering, Khalifa University of Science and Technology, Abu Dhabi, United Arab Emirates

ARTICLE INFO

Keywords:
Reactor containment building
Ultimate pressure capacity
Degradation
Rebar corrosion

ABSTRACT

Using ABAQUS, a non-linear finite element analysis (FEA) was performed to evaluate and compare the effects of degradation mechanisms by aging on the ultimate pressure capacity (UPC) of APR1400 reactor containment building (RCB). As the primary degradation mechanisms, prestress loss, concrete aging, rebar corrosion, and liner corrosion were simulated in the modelling and calculations. The results for unaged reactor containment buildings showed that the failure sequence by the internal pressure build-up consisted of 4 stages and reinforcement yielding strain of reinforced concrete would be the most important factor governing the UPC of RCBs. Among the four degradation mechanisms, corrosion occurring on the outer and inner rebar layers was identified as the main degradation mechanism affecting most significantly the ultimate pressure capacity of the APR1400 reactor containment building.

1. Introduction

In the design of reactor containment buildings (RCBs) in nuclear power plants (NPPs), external events such as earthquake and internal events such as large break loss of coolant accidents (LBLOCA) are considered (IAEA, 1998). In such accidental cases, RCBs in NPPs play a role as the last barrier to the release of radioactive materials to the environment (Lee, 2011; Mishra et al., 2016; Sharma et al., 2017). The consequences of some major nuclear accidents we experienced have shown the importance of the structural integrity of RCBs. Recently, severe accidents occurred in the Fukushima Daiichi power plants by the 2011 Tohoku earthquake and resulting tsunami (Gauntt et al., 2012). During the accidents, the RCBs of Units 1 and 3 suffered from combustible gas explosion and destruction of portions of the buildings, resulting in the release of large amounts of radioactive materials. However, in the Three Mile Island Unit 2 (TMI-2) reactor, its containment building remained intact and held almost all of the radioactive material released during the accident (U.S. Nuclear Regulatory Commission, 2013). The structural integrity of an RCB under internal pressurization from the design-basis accident and beyond design-basis accidents can be quantified by the ultimate pressure capacity (UPC) (Basha et al., 2003; Braverman et al., 2010; Chakraborty et al., 2017; Tavakkoli et al., 2017). On the other hand, the UPC of RCBs are significantly affected by aging (U.S. Nuclear Regulatory Commission, 2000; Sandia National Laboratories, 2000). Reviewing the documented performance of the 70 concrete containments in the USA, Shah and Hookham (1998) identified primary degradation mechanisms, which can be categorized as: i) aggressive chemical attack, ii) alkali–aggregate reactions, iii) leaching, iv) corrosion of reinforcing and pre-stressing steels, and v) stress relaxation of pre-stressing steel.

Many studies have been performed on the effect of some individual degradation mechanisms on the structural integrity of RCBs. The effect of a loss of pre-stress on the structural behavior and integrity of RCBs has been extensively studied (Lang and Wienand, 2013; Hu and Lin, 2016; Huang et al., 2017; Balomenos and Pandey, 2017). Also, the effect of liner corrosion on the failure of RCBs has been investigated (Sandia National Laboratories, 2000; Petti et al., 2008). However, the relative effects of different degradation mechanisms on the UPC of RCBs have not been fully addressed in literature. In this study, the effects of the primary degradation mechanisms on the UPC of the APR1400 RCBs were evaluated through calculating their UPC values under unaged and aged conditions. The UPC values were calculated by a nonlinear analysis using a three dimensional (3D) finite element model of one-quarter segment of the RCB (Barbat et al., 1998; U.S. Nuclear Regulatory Commission, 2010). By simulating the aged conditions for each degradation mechanism in the calculation, its effect on the UPC was evaluated and compared. Finally, the failure sequence of RCBs by internal pressure build-up as well as the most significant degradation mechanism affecting the UPC are discussed.

---

* Corresponding author at: PO Box 112021, Abu Dhabi, United Arab Emirates.
E-mail address: yongsun.yi@ku.ac.ae (Y. Yi).

https://doi.org/10.1016/j.nucengdes.2018.05.017
Received 27 March 2018; Received in revised form 13 May 2018; Accepted 15 May 2018

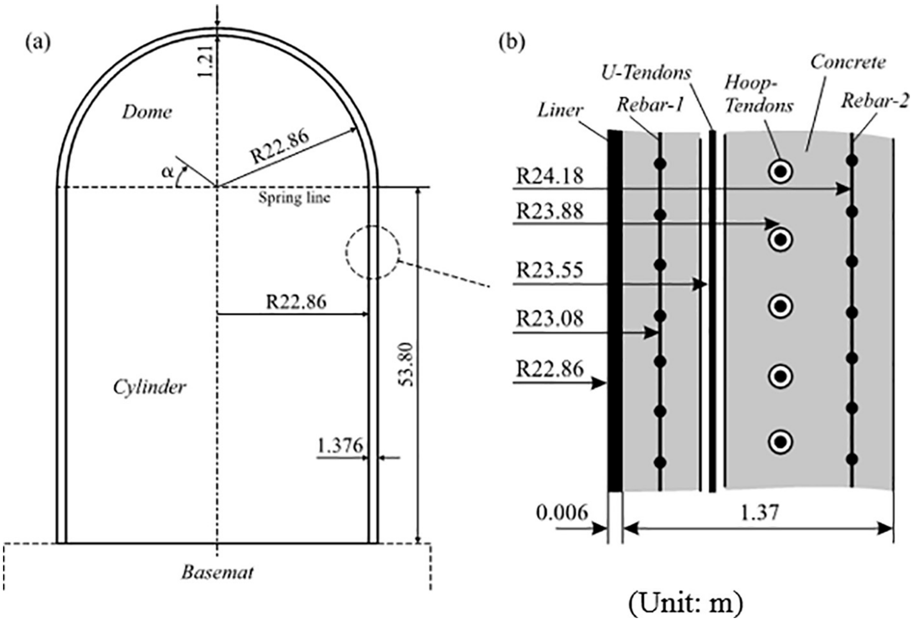

Fig. 1. Geometry of reactor containment building of APR1400.

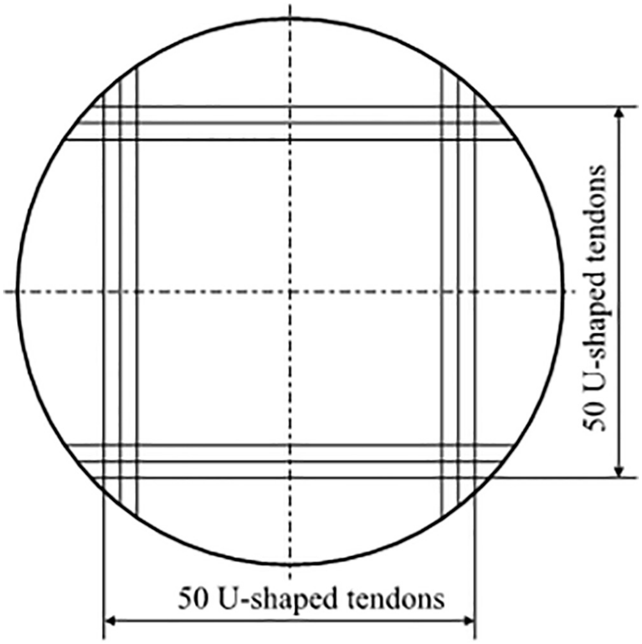

Fig. 2. Simplified geometry of reactor containment building of APR1400.

2. Finite element modelling

2.1. Containment geometry

The APR1400 PWR RCBs consists of a circular basemat foundation, an upright cylinder and a hemispherical dome (KEPCO, 2014). In addition, there are penetrations in the cylindrical concrete wall of the reactor containment building including equipment hatch, two personal airlocks, main stream lines, etc. Three buttresses are included in the reactor containment building to allow anchoring and tensioning of the tendons in the hoop direction while two groups of perpendicular U-shaped tendons are used to achieve the desired compressive axial prestress in the concrete wall. A simplified sketch of the APR 1400 RCB is shown in Fig. 1(a). The arrangement of structural components inside the containment wall and dome varies along the height of the RCB. An example of the structural configuration at mid-height of the containment wall is illustrated in Fig. 1(b). Two layers of reinforcing steels are embedded in the concrete wall and reinforcing steels are oriented along the axial and hoop directions in each layer. The interior surface of the containment is lined with a 6 mm thick steel liner to provide leak-tightness. The RCB is pre-stressed by a post-tensioning system with hoop tendons and inverted U-shaped tendons, as shown in Fig. 1(b) and Fig. 2.

In this study, we used the commercial FE software ABAQUS to generate a simplified geometric model of the APR 1400 RCB, omitting all penetrations (e.g. equipment hatch, airlocks, etc.) and buttresses. This can be justified by referring to the study of Shunmugavel and Gurbez (1987) who evaluated the UPCs of five types of pre-stressed concrete containments and found that the failure pressure of equipment hatch area was 30% greater compared to other failure modes. More recently, Cherry and Smith (2000) showed that the hatch region of the APR 1400 RCB appeared to be stiffer than other areas in the containment due to the high number of reinforcing steel bars placed around the penetrations. Furthermore, Chakraborty et al. (2017) observed that the presence of the basemat did not significantly influence the behaviour of the containment structure, which is consistent with an earlier investigation by Barbat et al. (1998). Therefore, the basemat was not explicitly included in our FE models. Instead, the containment wall was assumed to be rigidly connected to the ground. It was also assumed that the configuration of structural components in the RCB wall (rebar, tendons, and liner) would be uniform along the height of the containment wall.

Table 1
Summary of tendon and rebar geometry with dimensions (KEPCO, 2014).

	Direction	Layer	Diameter [m]	Spacing
Rebar	Meridional (Dome & Cylinder)	Inside	0.057	0.85°
		Outside	0.10	0.85°
	Hoop (Cylinder)	Inside	0.10	0.305 m
		Outside	0.057	0.305 m
	Hoop (Dome)	Inside	0.10	0.88°
		Outside	0.057	0.88°
Tendons	U-shaped (Dome & Cylinder)		0.015	0.72 m
	Hoop (Cylinder)		0.015	0.305 m
	Hoop (Dome)		0.015	0.88°